Original Article
Validation of a spatial normalization method using a principal component derived adaptive template for [18F]florbetaben PET

Antoine Leuzy[1], Kerstin Heurling[2], Susan De Santi[3], Santiago Bullich[3], Oskar Hansson[1,4], Johan Lilja[1,5,6]

[1]Clinical Memory Research Unit, Department of Clinical Sciences, Lund University, Malmö, Sweden; [2]Antaros Medical, Mölndal, Sweden; [3]Life Molecular Imaging Inc, Boston, MA, USA; [4]Memory Clinic, Skåne University Hospital, Lund, Sweden; [5]Hermes Medical Solutions, Stockholm, Sweden; [6]Department of Surgical Sciences, Nuclear Medicine and PET, Uppsala University, Uppsala, Sweden

Abstract: Quantification may help in the context of amyloid-β positron emission tomography (PET). Quantification typically requires that PET images be spatially normalized, a process that can be subject to bias. We herein aimed to test whether a principal component approach (PCA) previously applied to [18F]flutemetamol PET extends to [18F]florbetaben. PCA was applied to [18F]florbetaben PET data for 132 subjects (70 Alzheimer dementia, 62 controls) and used to generate an adaptive synthetic template. Spatial normalization of [18F]florbetaben data using this approach was compared to that achieved using SPM12's magnetic resonance (MR) imaging driven algorithm. The two registration methods showed high agreement and minimal difference in standardized uptake value ratios (SUVR) (R^2 = 0.997 using cerebellum as reference region and 0.996 using the pons). Our method allows for robust and accurate registration of [18F]florbetaben images to template space, without the need for an MR image, and may prove of value in clinical and research settings.

Keywords: Alzheimer's disease, Amyloid-β, PET, [18F]florbetaben, adaptive template

Introduction

Fibrillar amyloid-β (Aβ) plaques are a histological hallmark of Alzheimer's disease (AD) [1] and can be quantified in vivo using the carbon-11 labelled Thioflavin-T derivative Pittsburgh compound-B ([11C]PIB), and related fluorine-18 compounds, including [18F]flutemetamol [2, 3], [18F] florbetapir [4, 5] and [18F]florbetaben [6, 7]. These PET ligands are approved for clinical use by the Food and Drug Administration and European Medicines Agency and have been shown to be of value with respect to diagnostic confidence and patient management in clinical routine practice [8].

At present, only visual assessment of uptake is approved, whereby an Aβ PET scan is classified as either negative (normal) or positive (abnormal) by a trained rater. Evidence suggests, however, that the incorporation of quantitative approaches may improve agreement across raters [9] and aid in the monitoring of treatment effects in anti-Aβ trials [10]. The most common of these approaches is the use of a standardized uptake value ratio (SUVR), a semi-quantitative method involving the normalization of tracer uptake within cortical regions by that within a reference tissue, such as the cerebellum or pons [11]. A requisite for the computation of SUVRs is the demarcation of anatomical regions of interest (ROIs) and the gold standard for this relies on the use of high resolution T1-weighted magnetic resonance (MR) imaging. However, access to MR is often limited in clinical settings, and, in elderly individuals, contraindications for MR imaging are not uncommon [12]. Consequently, PET driven approaches have been developed, using probabilistic regional atlases [13].

A challenge inherent to [18F]-labelled Aβ ligands is that nonspecific binding to white matter is seen regardless of cortical Aβ levels. As a

result, uptake patterns across images can result in a systematic bias when a PET driven registration method is used. In an attempt to address this problem, we recently developed an automated PET only registration method using an adaptive template derived from a principal decomposition of [18F]flutemetamol PET images [14]. As this method allows for robust and accurate normalization of [18F]flutemetamol images without the need for MRI, it may simplify the clinical use of quantification with Aβ PET. In the present study we here aimed to validate this approach using [18F]florbetaben PET given its approval for commercial use and due to previous findings showing differences in cortical and white matter retention between [18F]flutemetamol and [18F]florbetaben [15, 16].

Materials and methods

Subjects

The study population consisted of 132 subjects from an open-label, multicenter non-randomized phase 2 clinical study [17]. 70 subjects had a clinical diagnosis of probable AD, based on the National Institute of Neurological and Communicative Diseases and Stroke-Alzheimer's Disease and Related Disorders Association (NINCDS-ADRDA) criteria and the revised Diagnostic and Statistical Manual of Mental Disorders IV [18, 19]. The remaining 62 subjects were cognitively unimpaired healthy controls, as indexed by a clinical dementia rating (CDR) score of zero, a Mini-Mental Status Examination (MMSE) score ≥ 28 and a z-score ≥ -1.00 for each subject of the CERAD neuropsychological test battery [20]. Controls also underwent structural brain scans with MR imaging; these were judged as "age-appropriate (normal)" and included ratings of cerebral atrophy [21] and cerebrovascular disease [22]. All participants provided written, informed consent. Our study was done in accordance with the Declaration of Helsinki after approval of the local ethics committees and radiation protection authorities of all participating centers.

Adaptive template generation

First, [18F]florbetaben images were co-registered to their corresponding MR images and spatially normalized to the Montreal Neurological Institute T1 template using the MR driven approach included in SPM12 (http://www.fil.

ion.ucl.ac.uk/spm). This approach allows for a global deformation field using a linear combination of low-frequency basis functions. Two sets of SUVR images were then created using a composite cortical region-encompassing brain regions typically showing high Aβ load in AD, including frontal, temporal and parietal cortices, precuneus, anterior striatum, and insular cortex-and the pons and cerebellar cortex as reference tissues [23]. Complete details pertaining to the creation of the synthetic template can be found in the original publication [14]. In brief, principal component images were calculated by singular value decomposition of the SUVR images for all subjects. A synthetic template, $I_{Synthetic}$, could then be modelled by a linear combination of the first principal component image, I_{PC1}, and the second principal component image, I_{PC2}, according to:

$$I_{Synthetic} = I_{PC1} + w\, I_{PC2}$$

where a negative value of w generates a template with an appearance towards the Aβ-negative range and a positive value of w generates a template with an appearance towards the Aβ-postive appearance. The synthetic [18F]florbetaben template could now be utilized by the registration algorithm described in the original publication [14] which incorporates both the weight (w) and parameters for spatial transformation in the optimization. This allows the registration method to iteratively find the best set of spatial transformation parameters for a given patient's [18F]florbetaben scan to fit the optimal template for this particular scan. Once converged, refinement of the registration of the brainstem and cerebellum is performed.

Refined reference region registration

Due to the low spatial resolution of PET, a refined local rigid-body registration approach was implemented for the pons and cerebellum. A binary mask covering the brain stem and cerebellum was first created. The binary mask was then smoothed using a 3-dimensional Gaussian kernel. The voxel intensities of the smoothed mask were then used as weights for the local rigid-body registration; a zero-value voxel of the smoothed mask hence leaves the corresponding voxel in the subject's image unaffected, while a voxel with value one will give a full contribution of the calculated rigid-body transform. This ensures that there are no discontinuities in the final registered image.

Table 1. Demographic variables for the study cohort

	AD	Controls	$P*$
N	70	62	
Age, years	70.07 ± 7.68	68.10 ± 6.58	..
Female, N (%)	31 (44%)	37 (60%)	..
Education (years)	12.39 (7.68)	14.54 (3.56)	..
MMSE	22.64 (2.61)	29.26 (0.77)	< 0.001
Word-list memory	10.76 (5.02)	22.53 (3.70)	< 0.001
Word-list recall	2.27 (2.11)	7.95 (1.65)	< 0.001

Data is presented as mean ± standard deviation or as n (%). MMSE = mini-mental state examination. *Group differences were tested for significance with the two-sided Fisher test for ordinal and the Wilcoxon test for continuous variables. .. = No significant difference between groups.
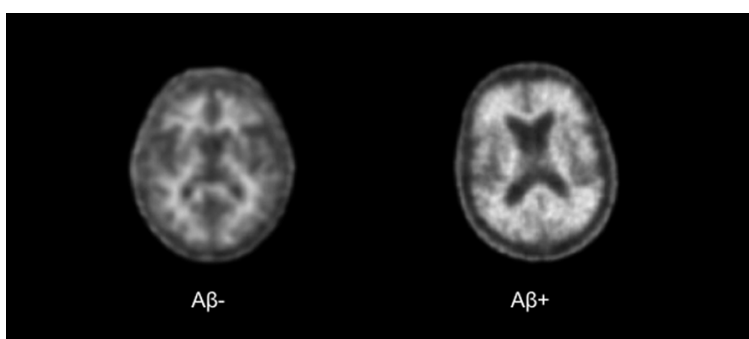

Figure 1. Representative coronal [18F]florbateben images showing an Aβ-negative (left) and an Aβ-positive (right) scans.

Spatial normalization and comparison with MR based registration

After co-registration to their corresponding MR scans, [18F]florbetaben images were spatially normalized to template space using two approaches: first, using spatial transforms derived from the MR driven registration in SPM12 and, second, using the principal component template registration method. In order to evaluate our method, coefficients of determination (R^2) were calculated between SUVR values derived using the principal component template and the SPM12 MR driven registration method. Absolute differences between SUVR values were also calculated using both approaches.

Results

Table 1 shows the main demographic variables for the study population. Spatial normalization was successfully achieved for all [18F]florbetaben images, with no manual corrections required. Representative [18F]florbetaben images are shown in **Figure 1**. Comparison of quan-

tification results using the [18F]florbetaben-driven principal component generated adaptive template registration and MR-driven SPM12 registration showed good agreement, with high R^2 values using both the cerebellum (0.997, P < 0.001) and pons (0.996, P < 0.001) as reference regions (**Figure 2**). Mean absolute differences between SUVRs calculated using both methods were low using the cerebellar cortex (AD = 1.702%, controls = 1.843%) and pons (AD = 1.724%, controls = 1.659%). The first and second principal component derived images, corresponding approximately to the average of all images and the difference between Aβ-positive and Aβ-negative images, are shown in **Figure 3A** and **3B**, respectively, with a selection of generated adaptive templates shown in **Figure 3C**.

Discussion

Building on the previous publication [14], in which the proposed PET driven adaptive template registration method was originally described using [18F]flutemetamol, we here show that our approach works equally well using [18F] florbetaben PET and a similar population.

In light of recent findings that clearly support Aβ imaging having a significant impact on the clinical management of patients with mild cognitive impairment or dementia [24], the clinical use of Aβ PET is likely to increase. Though currently available commercial Aβ tracers are approved for visual reads only, relevant levels of variability in both rater accuracy and between-reader agreement have been reported [25, 26]. While this topic has yet to be sufficiently explored, there is increasing evidence to suggest, increasing evidence to suggest that quantitation should be added to visual read in certain situations (e.g. inexperienced reader, borderline scans) [27]. Existing data indicates that quantitation improves both metrics [9, 28] with several commercial software packages available to calculate SUVRs, for example. Au-
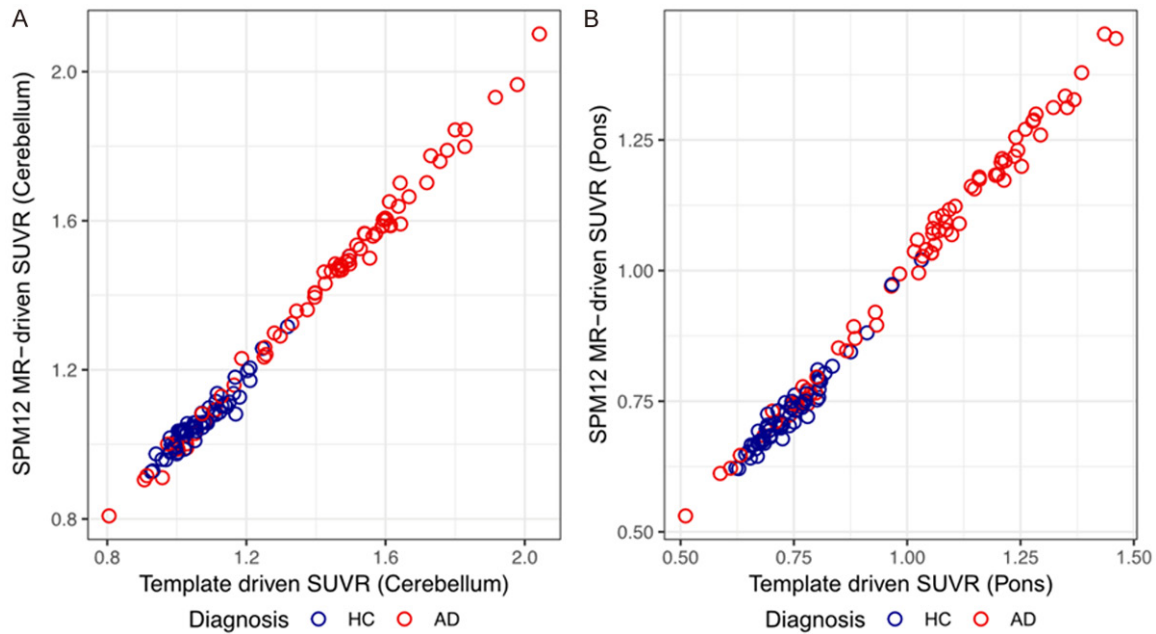
Figure 2. Scatterplot showing the comparison of [18F]florbateben SUVR values between PCA and SPM12 driven approaches using the cerebellum (A) and pons (B) as reference regions. R^2 values (P < 0.001): cerebellum, 0.997; pons, 0.996. HC = healthy controls, AD = Alzheimer's disease dementia.
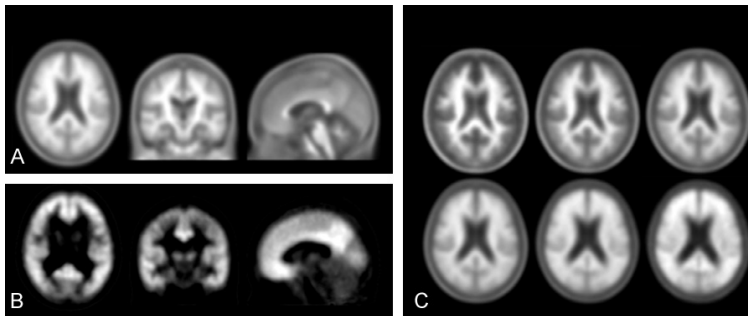

Figure 3. The first and second principal components are shown in (A) and (B); these represent, respectively, the average of all images and the difference between between Aβ-positive and negative images. Synthetic template images showing characteristic [18F]florbetaben uptake pattern going from most negative (upper left) to most positive case (lower right) are shown in (C).

tomated quantitation using the proposed registration method may thus aid in increasing reader certainty and further the clinical adoption of Aβ imaging, including within the context of future clinical trials testing anti-Aβ compounds in individuals who are Aβ PET negative but whose brain Aβ levels are rising [29]. Furthermore, as the proposed method performs as well as SPM12's MR based approach, it may simplify study protocols by removing the requirement for a separate T1-MR scan.

By comparison to other existing methods that employ adaptive [30] and principal component derived templates [31] for use with Aβ PET data, our approach carries a low computation cost (~20 seconds to process a single scan, as compared to > 6 hours for the method by Fripp and colleagues) and appears to generate a more accurate template. In addition, by contrast to the method developed Lundqvist and colleagues [30], for which a patent has been filed, our method is non-proprietary meaning that it can be easily distributed across interested parties within the field, potentially facilitating research into its application with Aβ tracers in different settings. As our primary focus is the potential use of this method in clinical settings, we have not evaluated our method using [11C]-Pittsburgh compound B ([11C]PiB) due its characteristic short half-life precluding its use clinically. As we have previously shown that our method works well with [18F]flutemetamol [14]-essentially the 18F-labelled version of PiB [32], with the two tracers shown to match closely in both controls and AD [33]-we think our method would work equally well with [11C]PiB. Though the availability of PET/MRI systems, allowing for the simultane-

ous acquisition of PET and MRI data, would circumvent the need for PET driven methods, the number of such platforms is quite low in comparison to stand-alone PET or PET/CT scanners [34].

Limitations of this study include the lack of neuropathological confirmation in subjects with a clinical diagnosis of probable AD. [18F]florbetaben PET, however, has previously been shown to have high sensitivity and specificity for detecting histopathology-confirmed neuritic Aβ plaque pathology [35]. Moreover, due the absence of cases with borderline changes that are difficult to classify visually, we were unable to examine the added benefit of our adaptive template method, and quantification in general, over visual read; this is, however, the subject of ongoing work using larger data sets. In addition, we did not assess the performance of our method in patients with non-AD neurodegenerative disorders such as frontotemporal lobar degeneration, which can be characterized by marked focal atrophy [36]. Finally, future studies are also required to address the extent to which the proposed method may apply to other PET tracers, including those for tau.

Conclusion

Our findings validate those originally reported for [18F]flutemetamol PET, indicating that the proposed method, which allows for a robust and accurate PET driven normalization procedure, applies equally well to [18F]florbetaben. The proposed method stands as a promising strategy that may simplify the implementation of quantification in clinical settings.

Future studies are required to address this and the extent to which this method may apply to other PET tracers, including those for tau.

Disclosure of conflict of interest

None.

Address correspondence to: Drs. Antoine Leuzy and Johan Lilja, Clinical Memory Research Unit, Department of Clinical Sciences, SE-205 02, Malmö, Sweden. Tel: +46 (0)462229667; E-mail: antoine. leuzy@med.lu.se (AL); Tel: +46 (0)40331000; johan. lilja@med.lu.se (JL)

References

[1] Mirra SS, Heyman A, McKeel D, Sumi SM, Crain BJ, Brownlee LM, Vogel FS, Hughes JP, van Belle G and Berg L. The consortium to establish a registry for alzheimer's disease (CERAD). Part II. Standardization of the neuropathologic assessment of Alzheimer's disease. Neurology 1991; 41: 479-486.

[2] US Food and Drug Administration. FDA approves second brain imaging drug to help evaluate patients for Alzheimer's disease, dementia. 2013.

[3] European Medicines Agency. Vizamyl: flutemetamol (18F). 2014. http://www.ema.europa.eu/docs/en_GB/document_library/ EPAR_-_Product_Information/human/002557/WC500172950.pdf.

[4] US Food and Drug Administration. FDA approves imaging drug Amyvid: estimates brain amyloid plaque content in patients with cognitive decline. 2012.

[5] European Medicines Agency. Amyvid: florbetapir (F). 2013.

[6] US Food and Drug Administration. FDA approves a second amyloid imaging agent. 2013.

[7] European Medicines Agency. Neuraceq: florbetaben (18F) Amyvid: florbetapir (18F). 2014.

[8] Fantoni ER, Chalkidou A, JTO Brien, Farrar G and Hammers A. A systematic review and aggregated analysis on the impact of amyloid PET Brain imaging on the diagnosis, diagnostic confidence, and management of patients being evaluated for alzheimer's disease. J Alzheimers Dis 2018; 63: 783-796.

[9] Nayate AP, Dubroff JG, Schmitt JE, Nasrallah I, Kishore R, Mankoff D and Pryma DA; Alzheimer's Disease Neuroimaging Initiative. Use of standardized uptake value ratios decreases interreader variability of [18F] florbetapir PET brain scan interpretation. AJNR Am J Neuroradiol 2015; 36: 1237-1244.

[10] Schmidt ME, Chiao P, Klein G, Matthews D, Thurfjell L, Cole PE, Margolin R, Landau S, Foster NL, Mason NS, De Santi S, Suhy J, Koeppe RA and Jagust W; Alzheimer's Disease Neuroimaging Initiative. The influence of biological and technical factors on quantitative analysis of amyloid PET: points to consider and recommendations for controlling variability in longitudinal data. Alzheimers Dement 2015; 11: 1050-1068.

[11] Wong DF, Rosenberg PB, Zhou Y, Kumar A, Raymont V, Ravert HT, Dannals RF, Nandi A, Brasic JR, Ye W, Hilton J, Lyketsos C, Kung HF, Joshi AD, Skovronsky DM and Pontecorvo MJ. In vivo imaging of amyloid deposition in Alzheimer disease using the radioligand 18F-AV-45 (flor-

betapir [corrected] F 18). J Nucl Med 2010; 51: 913-920.

[12] Tell GS, Lefkowitz DS, Diehr P and Elster AD. Relationship between balance and abnormalities in cerebral magnetic resonance imaging in older adults. Arch Neurol 1998; 55: 73-79.

[13] Desikan RS, Segonne F, Fischl B, Quinn BT, Dickerson BC, Blacker D, Buckner RL, Dale AM, Maguire RP, Hyman BT, Albert MS and Killiany RJ. An automated labeling system for subdividing the human cerebral cortex on MRI scans into gyral based regions of interest. Neuroimage 2006; 31: 968-980.

[14] Lilja J, Leuzy A, Chiotis K, Savitcheva I, Sorensen J and Nordberg A. Spatial normalization of [(18)F]flutemetamol PET images utilizing an adaptive principal components template. J Nucl Med 2019; 60: 285-291.

[15] Landau SM, Thomas BA, Thurfjell L, Schmidt M, Margolin R, Mintun M, Pontecorvo M, Baker SL and Jagust WJ; Alzheimer's Disease Neuroimaging Initiative. Amyloid PET imaging in Alzheimer's disease: a comparison of three radiotracers. Eur J Nucl Med Mol Imaging 2014; 41: 1398-1407.

[16] Villemagne VL, Mulligan RS, Pejoska S, Ong K, Jones G, O'Keefe G, Chan JG, Young K, Tochon-Danguy H, Masters CL and Rowe CC. Comparison of 11C-PiB and 18F-florbetaben for Abeta imaging in ageing and Alzheimer's disease. Eur J Nucl Med Mol Imaging 2012; 39: 983-989.

[17] Barthel H, Gertz HJ, Dresel S, Peters O, Bartenstein P, Buerger K, Hiemeyer F, Wittemer-Rump SM, Seibyl J, Reininger C and Sabri O; Florbetaben Study Group. Cerebral amyloid-beta PET with florbetaben (18F) in patients with Alzheimer's disease and healthy controls: a multicentre phase 2 diagnostic study. Lancet Neurol 2011; 10: 424-435.

[18] American Psychiatric Association. Task Force on DSM-IV. Diagnostic and statistical manual of mental disorders: DSM-IV. Washington, DC: American Psychiatric Association, 1994.

[19] McKhann G, Drachman D, Folstein M, Katzman R, Price D and Stadlan EM. Clinical diagnosis of Alzheimer's disease: report of the NINCDS-ADRDA Work Group under the auspices of Department of Health and Human Services Task Force on Alzheimer's Disease. Neurology 1984; 34: 939-944.

[20] Welsh KA, Butters N, Mohs RC, Beekly D, Edland S, Fillenbaum G and Heyman A. The Consortium to Establish a Registry for Alzheimer's Disease (CERAD). Part V. A normative study of the neuropsychological battery. Neurology 1994; 44: 609-614.

[21] Scheltens P, Leys D, Barkhof F, Huglo D, Weinstein HC, Vermersch P, Kuiper M, Steinling M, Wolters EC and Valk J. Atrophy of medial temporal lobes on MRI in "probable" Alzheimer's disease and normal ageing: diagnostic value and neuropsychological correlates. J Neurol Neurosurg Psychiatry 1992; 55: 967-972.

[22] Wahlund LO, Barkhof F, Fazekas F, Bronge L, Augustin M, Sjögren M, Wallin A, Ader H, Leys D, Pantoni L, Pasquier F, Erkinjuntti T and Scheltens P; European Task Force on Age-Related White Matter Changes. A new rating scale for age-related white matter changes applicable to MRI and CT. Stroke 2001; 32: 1318-1322.

[23] Klunk WE, Koeppe RA, Price JC, Benzinger TL, Devous MD Sr, Jagust WJ, Johnson KA, Mathis CA, Minhas D, Pontecorvo MJ, Rowe CC, Skovronsky DM and Mintun MA. The centiloid project: standardizing quantitative amyloid plaque estimation by PET. Alzheimers Dement 2015; 11: 1-15, e11-14.

[24] Rabinovici GD, Gatsonis C, Apgar C, Chaudhary K, Gareen I, Hanna L, Hendrix J, Hillner BE, Olson C, Lesman-Segev OH, Romanoff J, Siegel BA, Whitmer RA and Carrillo MC. Association of amyloid positron emission tomography with subsequent change in clinical management among medicare beneficiaries with mild cognitive impairment or dementia. JAMA 2019; 321: 1286-1294.

[25] Kobylecki C, Langheinrich T, Hinz R, Vardy ER, Brown G, Martino ME, Haense C, Richardson AM, Gerhard A, Anton-Rodriguez JM, Snowden JS, Neary D, Pontecorvo MJ and Herholz K. 18F-florbetapir PET in patients with frontotemporal dementia and Alzheimer disease. J Nucl Med 2015; 56: 386-391.

[26] Frey KA. Amyloid imaging in dementia: contribution or confusion? J Nucl Med 2015; 56: 331-332.

[27] Barthel H, Seibyl J and Sabri O. Yes we can analyse amyloid images - now what? Eur J Nucl Med Mol Imaging 2017; 44: 822-824.

[28] Pontecorvo MJ, Arora AK, Devine M, Lu M, Galante N, Siderowf A, Devadanam C, Joshi AD, Heun SL, Teske BF, Truocchio SP, Krautkramer M, Devous MD Sr and Mintun MA. Quantitation of PET signal as an adjunct to visual interpretation of florbetapir imaging. Eur J Nucl Med Mol Imaging 2017; 44: 825-837.

[29] McMillan CT and Chetelat G. Amyloid "accumulators": the next generation of candidates for amyloid-targeted clinical trials? Neurology 2018; 90: 759-760.

[30] Lundqvist R, Lilja J, Thomas BA, Lotjonen J, Villemagne VL, Rowe CC and Thurfjell L. Implementation and validation of an adaptive template registration method for 18F-flutemetamol imaging data. J Nucl Med 2013; 54: 1472-1478.

[31] Fripp J, Bourgeat P, Raniga P, Acosta O, Ville-magne V, Jones G, O'Keefe G, Rowe C, Ourselin S and Salvado O. MR-less high dimensional spatial normalization of 11C PiB PET images on a population of elderly, mild cognitive impaired and Alzheimer disease patients. Med Image Comput Comput Assist Interv 2008; 11: 442-449.

[32] Heurling K, Leuzy A, Zimmer ER, Lubberink M and Nordberg A. Imaging beta-amyloid using [(18)F]flutemetamol positron emission tomography: from dosimetry to clinical diagnosis. Eur J Nucl Med Mol Imaging 2016; 43: 362-373.

[33] Mathis C, Lopresti B, Mason N, Price J, Flatt N, Wenzhu B, Ziolko S, DeKosky S and Klunk W. Comparison of the amyloid imaging agents [F-18]3'-F-PIB and [C-11]PIB in Alzheimer's disease and control subjects. J Nucl Med 2007; 48.

[34] Ehman EC, Johnson GB, Villanueva-Meyer JE, Cha S, Leynes AP, Larson PEZ and Hope TA. PET/MRI: where might it replace PET/CT? J Magn Reson Imaging 2017; 46: 1247-1262.

[35] Sabri O, Sabbagh MN, Seibyl J, Barthel H, Akatsu H, Ouchi Y, Senda K, Murayama S, Ishii K, Takao M, Beach TG, Rowe CC, Leverenz JB, Ghetti B, Ironside JW, Catafau AM, Stephens AW, Mueller A, Koglin N, Hoffmann A, Roth K, Reininger C and Schulz-Schaeffer WJ; Florbetaben Phase 3 Study Group. Florbetaben PET imaging to detect amyloid beta plaques in Alzheimer's disease: phase 3 study. Alzheimers Dement 2015; 11: 964-974.

[36] Whitwell JL, Jack CR Jr, Senjem ML and Josephs KA. Patterns of atrophy in pathologically confirmed FTLD with and without motor neuron degeneration. Neurology 2006; 66: 102-104.